

computers & fluids

www.elsevier.com/locate/compfluid

Computers & Fluids 37 (2008) 336-348

Development of PML absorbing boundary conditions for computational aeroacoustics: A progress review

Fang Q. Hu

Department of Mathematics and Statistics, Old Dominion University, Norfolk, VA 23529, USA

Available online 27 February 2007

Abstract

Recent advances in the development of perfectly matched layer (PML) as absorbing boundary conditions for computational aero-acoustics are reviewed. The PML methodology is presented as a complex change of variables. In this context, the importance of a proper space—time transformation in the PML technique for Euler equations is emphasized. A unified approach for the derivation of PML equations is offered that involves three essential steps. The three-step approach is illustrated in details for the PML of linear and non-linear Euler equations. Numerical examples are also given that include non-reflecting boundary conditions for a ducted channel flow and mixing layer roll-up vortices.

© 2007 Published by Elsevier Ltd.

1. Introduction

At artificial boundaries, it is necessary to apply non-reflecting boundary conditions. In computational fluid dynamics and computational aeroacoustics, non-reflecting boundary conditions are often formulated based on the one-dimensional characteristics of governing equations or the far field asymptotic solutions (see, e.g., [29,11,25, 2,28]). Another common approach is to add a buffer/sponge zone to the non-reflecting boundary in which the numerical solutions are damped or filtered (see, e.g., reviews in [19,6]). Perfectly matched layer (PML) is a new technique of developing non-reflecting boundary conditions by constructing modified governing equations that can absorb out-going waves at open computational boundaries.

Berenger proposed the first perfectly matched layer in 1994 for computational electro-magnetics [5]. The significance of the PML technique lies in the fact that the absorbing zone is theoretically reflectionless for multi-dimensional linear waves of any angle and frequency. As a result, PML zones, when applicable, are usually thin compared to most other buffer zone formulations. Berenger's original PML

E-mail address: fhu@odu.edu

formulation used split physical variables, which was later shown to be dynamically stable but only weakly well-posed [1]. However, subsequent studies showed that PML technique was equivalent to a complex change of variables in the frequency domain and the PML equations could in fact be formed in unsplit physical variables [7,10,31,30].

Extension of the PML technique to computational fluid dynamics and computational aeroacoustics started with the linearized Euler equations with a uniform mean flow. In [16], Berenger's technique was first applied directly to the linear Euler equations. It was shown that the resulting PML equations were indeed perfectly matched to the linearized Euler equations, i.e., the PML absorbing domain is theoretically reflectionless to the acoustic, vorticity and entropy waves. However, numerical instability was also observed in [16] and, later, instability waves were found in [26] for the initial PML formulation given in [16]. Subsequently, in [18], it was found that the instability of the initial PML formulation was due to the fact that there is an inconsistency in the phase and group velocities of the acoustic wave in the presence of a non-zero mean flow. The analysis in [18] suggested that a necessary condition for the PML technique to work was that all physical waves have consistent phase and group velocities. The same condition was also reached independently in [4]. Recognizing this, new formulations of PML have appeared in the literature [18,12,13,3]. For instance, in [18], a stable PML for the linearized Euler equations with a uniform mean flow was proposed. It employed a space—time transformation before applying the PML technique so that in the transformed coordinates all waves have consistent phase and group velocities. This has led to a dynamically stable and computationally effective absorbing boundary condition. Other equivalent treatments of the necessary space—time transformation were also presented independently in the PML formulations given in [12,13,3].

Further extensions of PML technique to the linearized Euler equations with non-uniform mean flows were carried out in [12,20]. In [20], it was shown that with a uni-directional non-uniform mean flow, it would again be possible to apply a proper space—time transformation, determined by the dispersion relations of the acoustic wave modes supported by the mean flow, so that all linear waves have consistent phase and group velocities. Stable PML equations were derived following such transformations. Most recently, the PML technique has been applied to the non-linear Euler [21] and non-linear Navier—Stokes equations [14].

In this paper, these recent progresses in the development of PML for computational aeroacoustics will be reviewed and an emerging method of formulating PML absorbing boundary conditions for the governing equations of fluid dynamics will be offered. This method would involve three steps. First, a proper space—time transformation is determined and applied to the governing equations to ensure a consistency in the phase and group velocities of the linear waves; second, the transformed equation is modified with a PML complex change of variable in the frequency domain; and third, the absorbing boundary condition is obtained by re-writing the frequency domain PML in the original physical space and time coordinates.

In the next section, the basics of PML methodology is presented through a complex change of variables and the importance of a proper space–time transformation in the derivation of PML equations is explained. At the end of the section, three essential steps in deriving PML equations are outlined. Then, in Sections 3 and 4, PML for the linear and non-linear Euler equations are derived following the three-step method, with numerical examples that validate the effectiveness of PML as non-reflecting boundary conditions.

2. PML methodology and proper space-time transformation

The PML technique can be viewed as a complex change of variable in the frequency domain [7,8,10,30]. For example, consider the construction of a vertical x-layer that terminates the open computational domain in the x direction. This will involve a PML complex change of variable for x as

$$x \to x + \frac{\mathrm{i}}{\omega} \int_{x_{-}}^{x} \sigma_{x} \, \mathrm{d}x \tag{1}$$

where $\sigma_x > 0$ is the absorption coefficient (a constant or a function of x) and x_0 is the location of the PML/Euler interface. To see why such a complex change of variable will introduce wave absorption, consider a wave ansatz of the form

$$e^{i(kx-\omega t)}$$
 (2)

where k is the wavenumber in the direction of x and ω is the frequency. Under transformation (1) and (2) becomes

$$e^{i(kx-\omega t)}e^{-\frac{k}{\omega}\int_{x_0}^x \sigma_x \, dx}$$
(3)

while the eigenvectors of the system remain unchanged [18]. As argued in [18,20], the second factor in expression (3), with a purely real exponent, indicates that the wave amplitude will decay exponentially in the PML zone if, and only if,

$$\frac{k}{\omega} \int_{x'}^{x} \sigma_x \, \mathrm{d}x > 0 \tag{4}$$

as the wave propagates from an arbitrary location x' in the PML zone. This means that the PML is absorbing for a wave that propagates to the right (x increasing) with $k/\omega > 0$ or propagates to the left (x decreasing) with $k/\omega < 0$. In other words, for the amplitude of the wave to be reducing (and not increasing) in the PML domain, the sign of k/ω or, equivalently, the phase velocity ω/k , should be consistent with the direction of wave propagation [18,4]. Since the direction of propagation of a dispersive wave is determined by the group velocity, this necessary condition has been expressed nicely in [4] as

$$\frac{k}{\omega} \frac{\mathrm{d}\omega}{\mathrm{d}k} > 0 \tag{5}$$

This can also be written equivalently as

$$c_{\rm ph}c_{\rm g} > 0 \tag{6}$$

where $c_{\rm ph}$ and $c_{\rm g}$ represent, respectively, the phase velocity, ω/k , and the group velocity, $d\omega/dk$.

Unfortunately, in the presence of a mean flow, the phase and group velocities of acoustic waves are not always consistent. Consider linear waves in the presence of a uniform mean flow. The dispersion relations of linear waves supported by the Euler equations can be found in closed forms

$$D_{\rm I}(\omega, k) = (\omega - Uk)^2 - k^2 - k_{\nu}^2 = 0$$
 (7)

for the acoustic waves and

$$D_{\rm II}(\omega, k) = \omega - Uk = 0 \tag{8}$$

for the vorticity and entropy waves, where k_y is the wavenumber in the y direction and U is the mean flow Mach number (in x direction). The dispersion relations (7) and (8) are shown in Fig. 1. Clearly, for the vorticity and entropy waves, given by D_{II} , both the phase and group velocities are the same as the mean flow U, and thus are consistent in their signs, as required by (6). For the acoustic waves, given by D_{II} , however, an inspection of the dispersion curves in

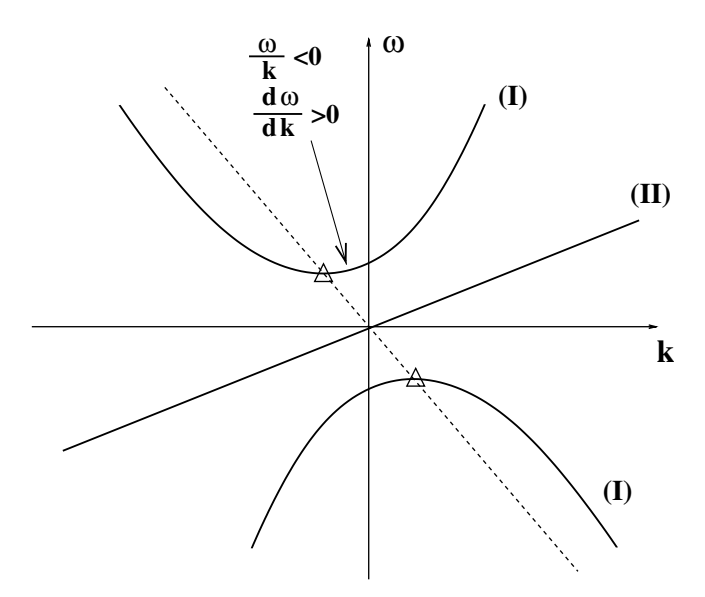


Fig. 1. Dispersion relations of the acoustic (I) and vorticity/entropy (II) waves. Symbols indicate the point of zero group velocity. The dashed line has a slope of $-(1-U^2)/U$.

Fig. 1 shows that there exist waves that have phase and group velocities in opposite directions. The points of zero group velocity are indicated by a triangle in Fig. 1. For the acoustic waves on the dispersion curve that are between the zero group velocity point and the vertical ω axis, their phase velocity is negative but their group velocity (slope of the dispersion curve) is positive. Therefore, if the PML technique is applied directly to the Euler equations, these waves will be amplified and give rise to instability of the layer. Thus, a modification of the Euler equation is needed before applying the PML complex change of variable (1).

The zero group velocity point (ω_0, k_0) of the acoustic waves can be found by solving coupled equations

$$D_{\mathbf{I}}(\omega_0, k_0) = 0 \tag{9}$$

$$\frac{\partial D_{\rm I}}{\partial k}(\omega_0, k_0) = 0 \tag{10}$$

By substituting (7) into (9) and (10), we find that, for any given value of k_{ν} ,

$$\frac{\omega_0}{k_0} = -\frac{1 - U^2}{U} \tag{11}$$

Since the ratio of ω_0 and k_0 is a fixed constant independent of k_y , it is now possible to apply a linear space—time transformation so that under the transformed coordinates, the phase and group velocities of all linear waves become consistent. For this purpose, a suitable transformation for a new time variable will be

$$\bar{t} = t + \beta x$$

which induces the following changes in the frequency and wavenumber space as

$$\bar{\omega} = \omega, \quad \bar{k} = k + \beta \omega$$
 (12)

By (11), the obvious choice for β is

$$\beta = -\frac{k_0}{\omega_0} = \frac{U}{1 - U^2} \tag{13}$$

It is straight forward to verify that, in the transformed coordinates, the dispersion relations (7) and (8) become

$$\bar{D}_{\rm I}(\bar{\omega},\bar{k}) = \frac{\bar{\omega}^2}{1 - U^2} - (1 - U^2)\bar{k}^2 - k_y^2 = 0 \tag{14}$$

for the acoustic waves and

$$\bar{D}_{II}(\bar{\omega},\bar{k}) = \frac{\bar{\omega}}{1 - U^2} - U\bar{k} = 0 \tag{15}$$

for the vorticity and entropy waves, as plotted in Fig. 2. Now all the waves have consistent phase and group velocities. Application of the PML technique in the transformed coordinates should now yield stable absorbing boundary conditions.

As we have seen, a proper space—time transformation plays an important role in the stability of PML for the Euler equations. In proceeding discussions, the value of β is determined from the dispersion relation of the acoustic waves, by (9), (10) and (13). If the mean flow is non-uniform, no closed-form dispersion relation is available and a numerical study on the dispersion relation of linear waves has to be carried out, as discussed in details in [20]. However, for the special case of constant mean density, i.e., when $\bar{\rho} = 1$, a simple empirical formula for β was given in [20], where

$$\beta = \frac{U_m}{1 - U_m^2}, \quad U_m = \frac{1}{b - a} \int_a^b \overline{U}(y) \, \mathrm{d}y$$
 (16)

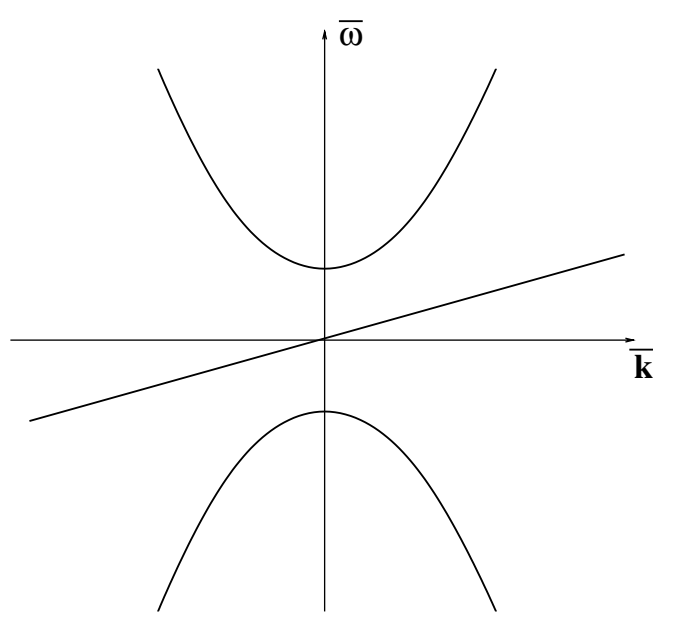


Fig. 2. Dispersion relations of the acoustic (I) and vorticity/entropy (II) waves in transformed coordinates.

in which $a \le y \le b$ is the computational domain for y and U_m is the average of mean velocity $\overline{U}(y)$. In summary, the derivation of PML equations for the Euler equations will involve essentially three steps:

Step 1, apply a proper space-time transformation,

$$\bar{t} = t + \beta x \tag{17}$$

This will result in the changes of partial derivative terms as

$$\frac{\partial}{\partial t} \to \frac{\partial}{\partial t}, \qquad \frac{\partial}{\partial x} \to \frac{\partial}{\partial x} + \beta \frac{\partial}{\partial t}$$
 (18)

Step 2, apply PML complex change of variables in the frequency domain of transformed variables,

$$x \to x + \frac{i}{\bar{\omega}} \int_{x_0}^x \sigma_x \, dx, \quad y \to y + \frac{i}{\bar{\omega}} \int_{y_0}^y \sigma_y \, dy,$$

$$z \to z + \frac{i}{\bar{\omega}} \int_{z_0}^z \sigma_z \, dz \tag{19}$$

for x–, y– and z–layers respectively, where σ_x , σ_y and σ_z are positive functions of x, y and z respectively. This will result in the changes of partial derivatives as

$$\frac{\partial}{\partial x} \to \frac{1}{1 + i \frac{\sigma_x}{\bar{\sigma}_x}} \frac{\partial}{\partial x}, \quad \frac{\partial}{\partial y} \to \frac{1}{1 + i \frac{\sigma_y}{\bar{\sigma}_y}} \frac{\partial}{\partial y},
\frac{\partial}{\partial z} \to \frac{1}{1 + i \frac{\sigma_z}{\bar{\sigma}_z}} \frac{\partial}{\partial z} \tag{20}$$

Step 3, re-write the frequency domain equations in the original space and time variables.

In the next two sections, this three-step method will be illustrated by examples of PML for the linear and non-linear Euler equations.

3. PML for linearized Euler equations

We consider the construction of PML equations as non-reflecting boundary conditions for a ducted Couette flow with a subsonic non-uniform mean velocity. This problem was one of those proposed in the fourth CAA workshop of Benchmark problems [9]. As shown in Fig. 3, non-reflecting boundary conditions are needed at the inflow and outflow boundaries of the channel. We will discuss the construction of stable PML equation following the three-step method described in the previous section.

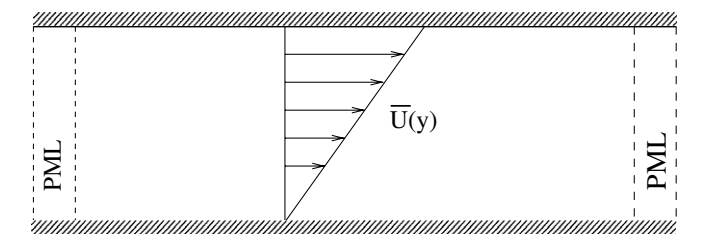


Fig. 3. Schematic of Couette flow with PML absorbing boundary condition.

3.1. Dispersion relation and determination of value for β

The linearized Euler equation with a non-uniform mean flow is

$$\frac{\partial \mathbf{u}}{\partial t} + \mathbf{A} \frac{\partial \mathbf{u}}{\partial x} + \mathbf{B} \frac{\partial \mathbf{u}}{\partial y} + \mathbf{C} \mathbf{u} = 0 \tag{21}$$

where

$$\mathbf{u} = \begin{pmatrix} \rho \\ u \\ v \\ p \end{pmatrix}, \quad \mathbf{A} = \begin{pmatrix} \overline{U} & 1 & 0 & 0 \\ 0 & \overline{U} & 0 & 1 \\ 0 & 0 & \overline{U} & 0 \\ 0 & 1 & 0 & \overline{U} \end{pmatrix}, \quad \mathbf{B} = \begin{pmatrix} 0 & 0 & 1 & 0 \\ 0 & 0 & 0 & 0 \\ 0 & 0 & 0 & 1 \\ 0 & 0 & 1 & 0 \end{pmatrix}, \quad \mathbf{C} = \begin{pmatrix} 0 & 0 & 0 & 0 \\ 0 & 0 & \frac{d\overline{U}}{dy} & 0 \\ 0 & 0 & 0 & 0 \\ 0 & 0 & 0 & 0 \end{pmatrix}$$

The mean velocity is given by $\widetilde{U}(y) = 0.9y$ in a physical domain of $-2 \le x \le 2$ and $0 \le y \le 1$. The mean density has been assumed to be constant, $\bar{\rho} = 1$. Solid wall boundary conditions are applied at y = 0 and y = 1.

To construct the PML equation for the Euler equations in (21) with a non-uniform mean flow, we first examine the physical waves associated with (21) and their dispersion relations. For this purpose, a dispersive wave analysis of (21) is carried out. Specifically, we let

$$\mathbf{u} = \hat{\mathbf{u}}(y)e^{\mathrm{i}(kx - \omega t)} \tag{22}$$

in (21) and get

$$-i\omega\hat{\mathbf{u}} + ik\mathbf{A}\hat{\mathbf{u}} + \mathbf{B}\frac{d\hat{\mathbf{u}}}{dv} + \mathbf{C}\hat{\mathbf{u}} = 0$$
 (23)

Together with the homogeneous boundary conditions at y = 0 and y = 1, (23) forms an eigenvalue problem for ω for any given value of k. The eigensolutions are called normal modes in the theory of hydrodynamic stability analysis. This eigenvalue problem has been solved numerically by a spectral collocation method using Chebyshev polynomials [20]. It yields a complete spectrum of the waves supported by (23).

Fig. 4 shows the dispersion relation diagram of all the normal modes of (23), i.e., real part of ω vs. k. The imaginary part of ω is found to be zero for all modes, indicating that the Couette flow does not have physical instability wave.

In the dispersion diagram, we see two families of waves. One family has phase speed between $U_{\min}=0$ and $U_{\max}=0.9$, shown between dashed lines in the ω_r -k diagram. These are "vortical" modes that convect with the mean flow. They are non-dispersive waves, i.e., $\omega/k=$ constant [32]. For these waves, condition (6) is satisfied.

The other family of modes are "acoustic" modes [27,23]. A closer examination of the acoustic modes indicates that they have a phase speed supersonic relative to part of the mean flow. They are dispersive waves. Fig. 4 indicates that the acoustic modes do not always have consistent phase and group velocities. A triangle on the acoustic modes denotes the location where the group velocity is zero. As we can see, for the acoustic modes in the upper left and lower right quarters in Fig. 6 that lie between the triangle

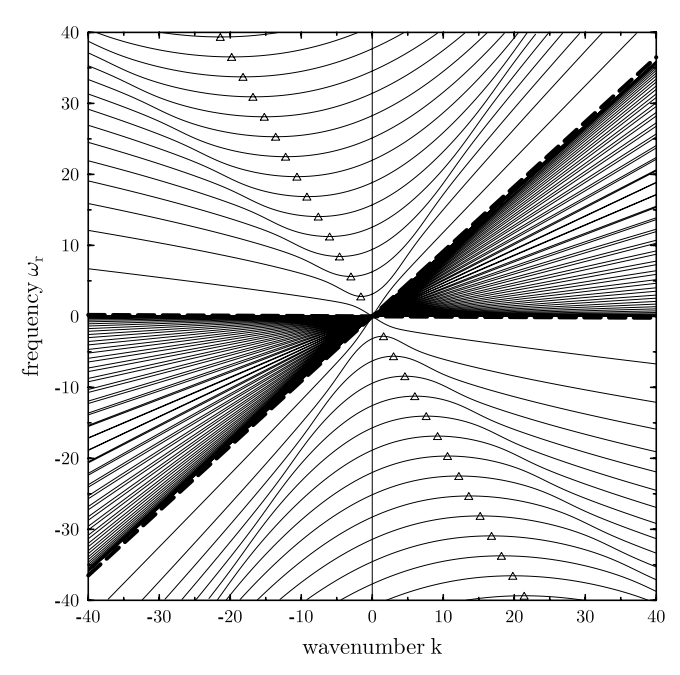


Fig. 4. Dispersion relation diagram of physical wave. Triangles denote the points of zero group velocity.

and the vertical axis, their phase velocity (ω_r/k) is negative but their group velocity $(d\omega_r/dk)$ is positive. This situation is quite similar to the case of uniform flow shown in Fig. 1. As has been explained earlier, applying the PML complex change of variable (1) to the Euler equations (21) without a proper space—time coordinate transformation will result in these waves being amplified and becoming unstable modes.

Remarkably, the locations of points of zero group velocity on the dispersion diagram (triangles in Fig. 4) appear to lie nearly on a straight line. Inspection of points of zero group velocity shows a line of $\omega_r = c_0 k$ where the slope of the line is approximately $c_0 = -1.85$. This suggests a space–time coordinate transformation of the form (17) with the value for β determined by

$$\beta = -\frac{1}{c_0} = 0.54\tag{24}$$

We point out that if the empirical formula (16) is directly used here, we have $U_m = 0.45$ and a value for $\beta = 0.56$, which is a very good approximation and could also be used effectively in computations. In Fig. 5, we show the dispersion relation diagram in frequency—wavenumber space of the transformed coordinates. Indeed, we see that the phase and group velocities of all waves are consistent and the necessary condition (6) becomes satisfied by all wave modes.

3.2. Derivation of PML equation

Once the value for β is determined, the derivation of PML equation can proceed as described in the previous section. In the first step, after the space-time transforma-

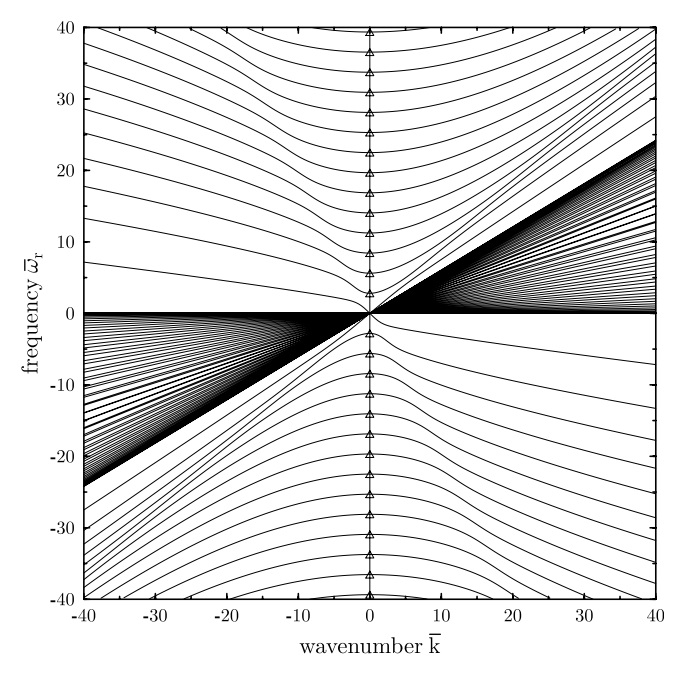


Fig. 5. Dispersion relation diagram after applying the space-time transformation.

tion (17), the Euler equations in the frequency domain becomes

$$-i\bar{\omega}(\mathbf{I} + \beta \mathbf{A})\tilde{\mathbf{u}} + \mathbf{A}\frac{\partial \tilde{\mathbf{u}}}{\partial x} + \mathbf{B}\frac{\partial \tilde{\mathbf{u}}}{\partial y} + \mathbf{C}\tilde{\mathbf{u}} = 0$$
 (25)

For the second step, by a complex change of variable of the form (19) for x, we get the following PML equations in the frequency domain,

$$-i\bar{\omega}(\mathbf{I} + \beta \mathbf{A})\tilde{\mathbf{u}} + \frac{1}{1 + \frac{i\sigma_x}{\tilde{\omega}}} \mathbf{A} \frac{\partial \tilde{\mathbf{u}}}{\partial x} + \mathbf{B} \frac{\partial \tilde{\mathbf{u}}}{\partial y} + \mathbf{C}\tilde{\mathbf{u}} = 0$$
 (26)

Finally, to re-write the above in the time domain, we multiply $1 + \frac{i\sigma_2}{\bar{\omega}}$ to the equation and get

$$(-i\bar{\omega} + \sigma_x)(\mathbf{I} + \beta \mathbf{A})\tilde{\mathbf{u}} + \mathbf{A}\frac{\partial \tilde{\mathbf{u}}}{\partial x} + \left(1 + \frac{i\sigma_x}{\bar{\omega}}\right)\mathbf{B}\frac{\partial \tilde{\mathbf{u}}}{\partial y} + \left(1 + \frac{i\sigma_x}{\bar{\omega}}\right)\mathbf{C}\tilde{\mathbf{u}} = 0$$
(27)

This can be readily re-written in the original physical time domain as follows:

$$\frac{\partial \mathbf{u}}{\partial t} + \mathbf{A} \frac{\partial \mathbf{u}}{\partial x} + \mathbf{B} \frac{\partial \mathbf{u}}{\partial y} + \sigma_x \mathbf{B} \frac{\partial \mathbf{q}}{\partial y} + \mathbf{C}(\mathbf{u} + \sigma_x \mathbf{q})
+ \sigma_x \mathbf{u} + \sigma_x \beta \mathbf{A} \mathbf{u} = 0$$
(28)

where

$$\frac{\partial \mathbf{q}}{\partial t} = \mathbf{u} \tag{29}$$

as shown in [18,20]. Here, **q** is an auxiliary variable vector. It is only needed inside the PML domain [18]. Eqs. (28) and (29) form the system of equations to be solved in the PML domains at the inflow and outflow boundaries.

3.3. Numerical example

For numerical results, a computational domain of $[-2.15625, 2.15625] \times [0, 1]$ will be used, which is discretized by a uniform grid of 553×129 points with $\Delta x = \Delta y = 1/128$ and 20 grid points in the PML domains at the inflow and outflow.

The initial conditions are the acoustic and density pulses given in the Benchmark problem [9]. The spatial derivatives are approximated by the 7-point DRP scheme [28] and the time integration is carried out by the optimized 5- and 6-stage alternating low-dissipation and low-dispersion Runge–Kutta scheme (LDDRK5-6 [22]). A 10th order filter has also been applied to limit the oscillations from the thin density wave in the problem.

The absorption coefficient in the PML domain varies with x as follows:

$$\sigma_x = \frac{4}{\Delta x} \left| \frac{x - x_0}{D} \right|^2 \tag{30}$$

where x_0 denotes the interface of the Euler and PML domains and D is the width of the PML domain, i.e., $D = 20\Delta x$ for the cases reported here.

A grid stretching inside the PML also improves the effectiveness of the PML because the total absorption rate depends directly on the width of the PML domain [19]. The grid stretching is equivalent to modifying the *x* derivative term of the PML equation as

$$\frac{\partial}{\partial x} \to \frac{1}{\alpha(x)} \frac{\partial}{\partial x} \tag{31}$$

where $\alpha(x) \ge 1$ is a smooth function with $\alpha(x_0) = 1$ [19]. We have used the following expression for $\alpha(x)$ in the calculations,

$$\alpha(x) = 1 + 2 \left| \frac{x - x_0}{D} \right|^2 \tag{32}$$

The initial acoustic pulse is reflected back and fourth by the channel walls and, at the same time, radiates outward through the inflow and outflow boundaries. Fig. 6 shows the pressure contours of the numerical and exact solutions at t = 8, 16 and 32. Because of the repeated reflections by channel walls, the out-going waves are propagating increasingly at a grazing angle with the boundary, a situation very difficult to treat using characteristics based boundary conditions. Under the present PML absorbing boundary condition, the numerical solution decays exponentially inside the PML domain with very little reflection. Even with only 20 grid points in the PML domain, the agreements on contours between the numerical and exact solutions are excellent. Fig. 7 shows the density contours. The absorption of the density pulse by the PML domain is clearly shown. We note that the initial density pulse is stretched thin by the shear mean flow and becomes less resolved by the 7-point finite difference scheme at t = 16 and beyond. Although there are some oscillations near the density wave, the overall contours compare well with the exact solution. Clearly, PML Eq. (28) can provide a very effective non-reflecting boundary condition for duct flows.

4. PML for non-linear Euler equations

In this section, we give an example of constructing PML for the two-dimensional non-linear Euler equation. Written in conservation form, the Euler equations are

$$\frac{\partial \mathbf{u}}{\partial t} + \frac{\partial \mathbf{F}_1(\mathbf{u})}{\partial x} + \frac{\partial \mathbf{F}_2(\mathbf{u})}{\partial y} = 0 \tag{33}$$

where

$$\mathbf{u} = \begin{bmatrix} \rho \\ \rho u \\ \rho v \\ \rho e \end{bmatrix}, \quad \mathbf{F}_1 = \begin{bmatrix} \rho u \\ \rho u^2 + p \\ \rho uv \\ \rho h u \end{bmatrix}, \quad \mathbf{F}_2 = \begin{bmatrix} \rho v \\ \rho uv \\ \rho v^2 + p \\ \rho h v \end{bmatrix}$$
(34)

....

$$h = e + \frac{p}{\rho}, \quad p = (\gamma - 1)\rho\left(e - \frac{u^2 + v^2}{2}\right)$$
 (35)

In (34) and (35), u and v are the velocity components, p is the pressure, ρ is the density and e is the energy. Specific heats ratio $\gamma = 1.4$.

At non-reflecting boundaries, we introduce PML domains to absorb out-going disturbances, as shown in Fig. 8. We wish to formulate the equations to be used in the PML domain so that the disturbances can be exponentially reduced once they enter the added zones.

In a non-linear simulation, the total variable **u** can be considered as consisting of a time independent mean state and a perturbation that has to be governed by non-linear equations. Since the mean state could be quite large compared to the time-dependent perturbed state, it may not be most efficient to absorb the total variable **u** and to reduce it to nearly zero inside the PML domain. Although it is common to decompose the total variable **u** into a time-independent mean-flow and a time-dependent fluctuation, the exact mean state is usually unknown at the start of the computation. The PML formulation presented here will not require the exact mean-flow. Instead, we shall partition the solution inside the PML domain into two parts as

$$\mathbf{u} = \bar{\mathbf{u}}_{-} + \mathbf{u}' \tag{36}$$

where $\bar{\mathbf{u}}_p$ is a time-independent "pseudo mean-flow" [17,21]. It is important to note that it is not necessary for this pseudo mean-flow to be the exact mean-flow at the non-reflecting boundary. We only require that the chosen $\bar{\mathbf{u}}_p$ satisfy the steady Euler equation:

$$\frac{\partial \mathbf{F}_{1}(\bar{\mathbf{u}}_{p})}{\partial x} + \frac{\partial \mathbf{F}_{2}(\bar{\mathbf{u}}_{p})}{\partial y} = 0 \tag{37}$$

The use of $\bar{\mathbf{u}}_p$ is strictly to make the PML domain more efficient since we now need only to absorb u', the difference

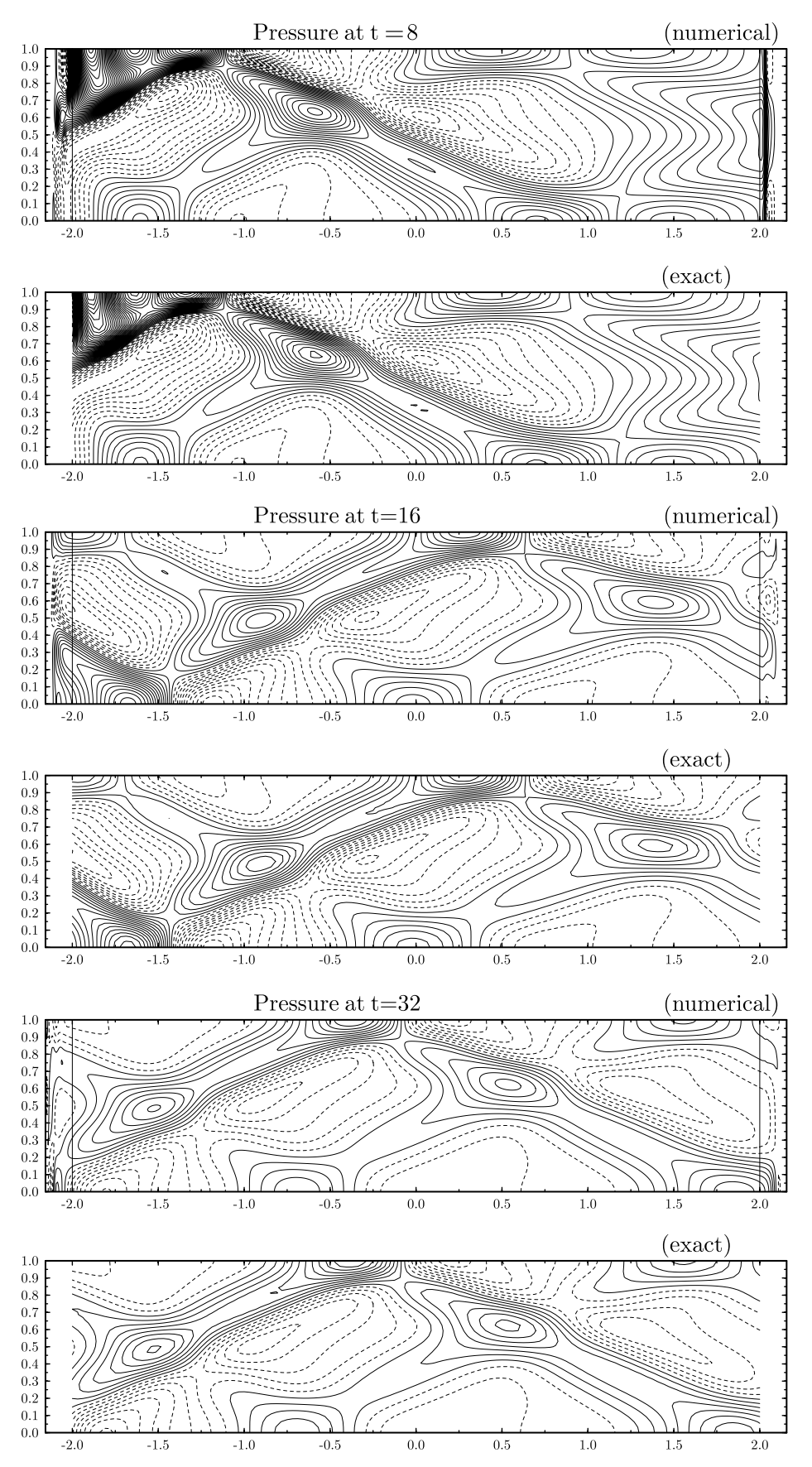


Fig. 6. Pressure contours at t = 8, 16 and 32.

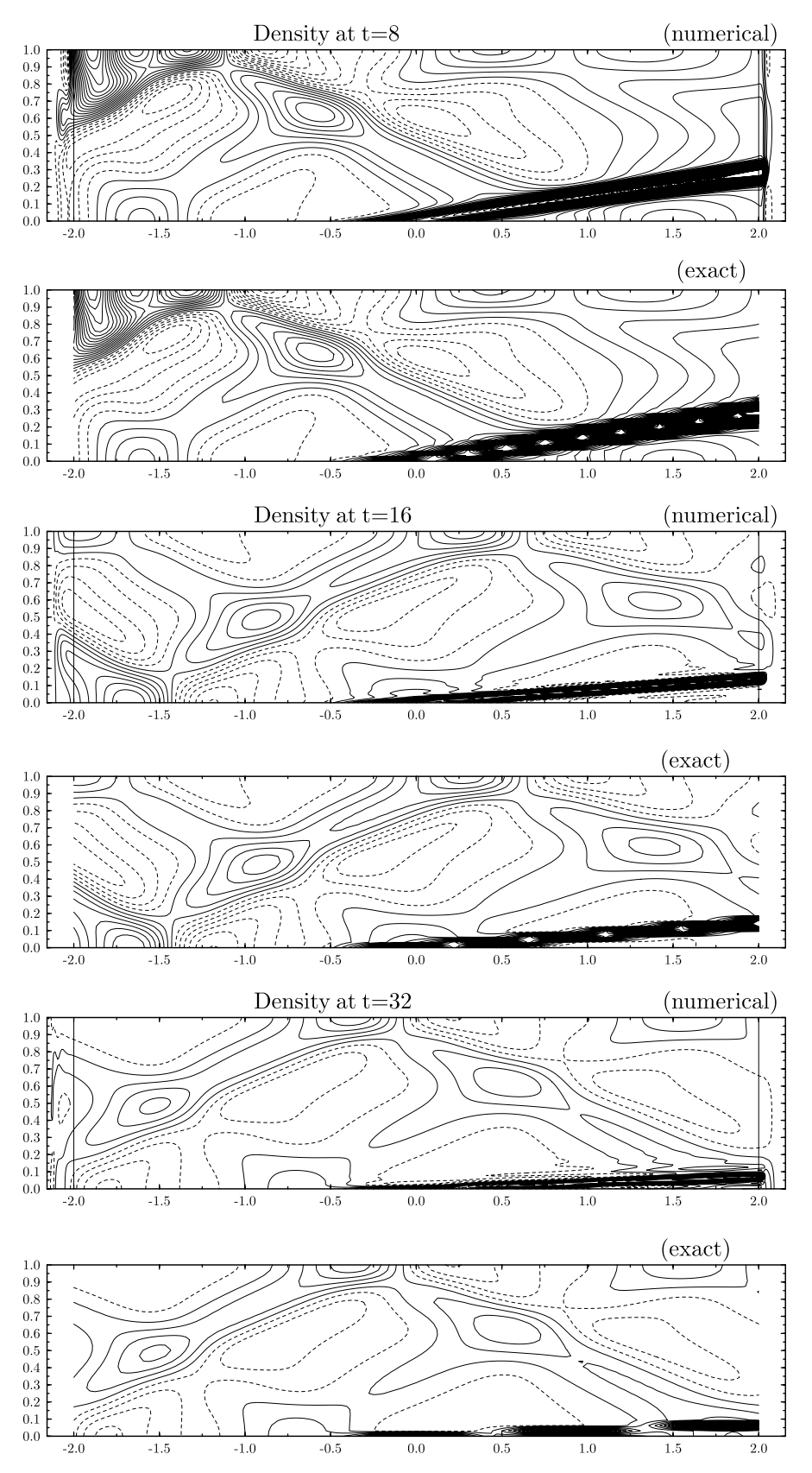


Fig. 7. Density contours at t = 8, 16 and 32.

between u and a prescribed pseudo mean-flow $\bar{\textbf{u}}_p$, as illustrated in Fig. 9. Obviously, the choice for $\bar{\textbf{u}}_p$ is not unique.

In what follows, we shall develop PML equations that absorb $u^\prime,$ the difference between u and \bar{u}_p inside the

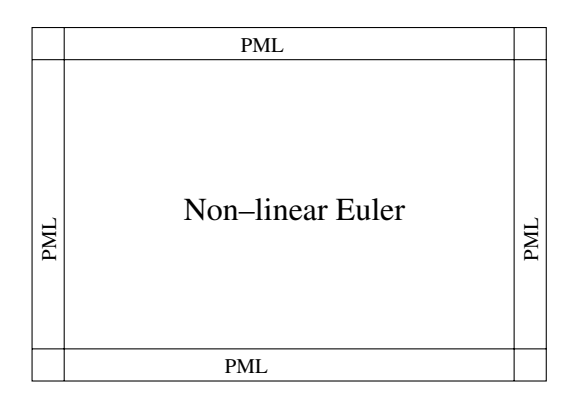


Fig. 8. Schematic of Euler and PML domains with four open boundaries.

PML domain. By Eq. (37), it is easy to see that the equation for \mathbf{u}' can be written as

$$\frac{\partial \mathbf{u}'}{\partial t} + \frac{\partial [\mathbf{F}_1(\mathbf{u}) - \mathbf{F}_1(\bar{\mathbf{u}}_p)]}{\partial x} + \frac{\partial [\mathbf{F}_2(\mathbf{u}) - \mathbf{F}_2(\bar{\mathbf{u}}_p)]}{\partial y} = 0$$
 (38)

Following the three-step method for the derivation of PML, we will first apply a proper space–time transformation of the form (17) to Eq. (38):

$$\frac{\partial \mathbf{u}'}{\partial \bar{t}} + \beta \frac{\partial [\mathbf{F}_{1}(\mathbf{u}) - \mathbf{F}_{1}(\bar{\mathbf{u}}_{p})]}{\partial \bar{t}} + \frac{\partial [\mathbf{F}_{1}(\mathbf{u}) - \mathbf{F}_{1}(\bar{\mathbf{u}}_{p})]}{\partial x} + \frac{\partial [\mathbf{F}_{2}(\mathbf{u}) - \mathbf{F}_{2}(\bar{\mathbf{u}}_{p})]}{\partial y} = 0$$
(39)

Here, the parameter β is based on the pseudo mean flow $\bar{\mathbf{u}}_p$ [21]. In the frequency domain, the above is

$$(-i\overline{\omega})(\tilde{\mathbf{u}}' + \beta[\mathbf{F}_{1}(\mathbf{u}) - \mathbf{F}_{1}(\bar{\mathbf{u}}_{p})]) + \frac{\partial[\mathbf{F}_{1}(\mathbf{u}) - \mathbf{F}_{1}(\bar{\mathbf{u}}_{p})]}{\partial x} + \frac{\partial[\mathbf{F}_{2}(\mathbf{u}) - \mathbf{F}_{2}(\bar{\mathbf{u}}_{p})]}{\partial y} = 0$$

$$(40)$$

where $\tilde{\parallel}$ denotes the time Fourier transformed quantity. As a second step, we apply the PML complex change of variables (19) to the above and get

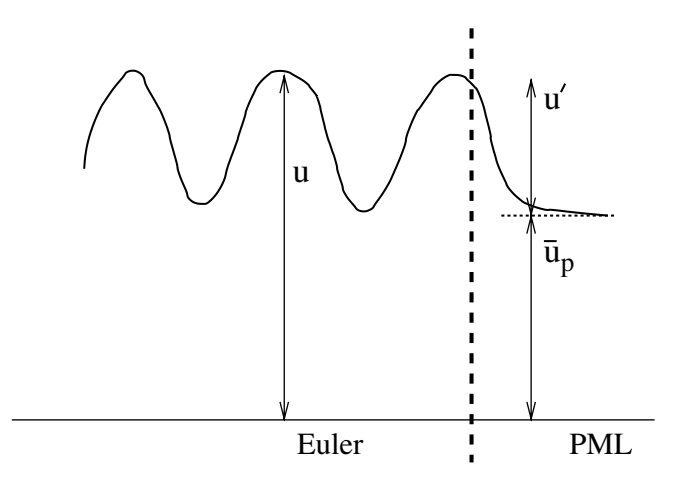


Fig. 9. Absorption of non-linear disturbances with a pseudo mean-flow in the PML domain.

$$\begin{split} &(-i\bar{\omega})(\tilde{\mathbf{u}}'+\beta[\mathbf{F}_{1}(\mathbf{u})\widetilde{-\mathbf{F}_{1}}(\bar{\mathbf{u}}_{p})])+\frac{1}{1+i\frac{\sigma_{x}}{\bar{\omega}}}\frac{\partial[\mathbf{F}_{1}(\mathbf{u})\widetilde{-\mathbf{F}_{1}}(\bar{\mathbf{u}}_{p})]}{\partial x} \\ &+\frac{1}{1+i\frac{\sigma_{y}}{\bar{\omega}}}\frac{\partial[\mathbf{F}_{2}(\mathbf{u})\widetilde{-\mathbf{F}_{2}}(\bar{\mathbf{u}}_{p})]}{\partial y}=0 \end{split} \tag{41}$$

Eq. (41) is the PML equation for (38) in the frequency domain. As a final step, we shall write (41) in the original time domain. We will present two approaches. The first uses unsplit physical variables while the second uses split equations but introduces fewer auxiliary variables.

4.1. Unsplit version

In the unsplit approach, following [12,14], we multiply $(1+i\frac{\sigma_x}{\bar{\omega}})(1+i\frac{\sigma_y}{\bar{\omega}})$ to Eq. (41) and get

$$\left(-i\overline{\omega} + \sigma_{x} + \sigma_{y} + i\frac{\sigma_{x}\sigma_{y}}{\overline{\omega}}\right)(\overline{\mathbf{u}}' + \beta[\mathbf{F}_{1}(\mathbf{u}) - \overline{\mathbf{F}}_{1}(\overline{\mathbf{u}}_{p})])
+ \left(1 + i\frac{\sigma_{y}}{\overline{\omega}}\right) \frac{\partial[\mathbf{F}_{1}(\mathbf{u}) - \overline{\mathbf{F}}_{1}(\overline{\mathbf{u}}_{p})]}{\partial x}
+ \left(1 + i\frac{\sigma_{x}}{\overline{\omega}}\right) \frac{\partial[\mathbf{F}_{2}(\mathbf{u}) - \overline{\mathbf{F}}_{2}(\overline{\mathbf{u}}_{p})]}{\partial y} = 0$$
(42)

By defining auxiliary variables \mathbf{q}_0 , \mathbf{q}_1 and \mathbf{q}_2 as

$$\frac{\partial \mathbf{q}}{\partial t} = \mathbf{u}',\tag{43}$$

$$\frac{\partial \mathbf{q}_1}{\partial \bar{t}} = \mathbf{F}_1(\mathbf{u}) - \mathbf{F}_1(\bar{\mathbf{u}}_p),\tag{44}$$

$$\frac{\partial \mathbf{q}_2}{\partial \bar{t}} = \mathbf{F}_2(\mathbf{u}) - \mathbf{F}_2(\bar{\mathbf{u}}_p), \tag{45}$$

the time domain equation for (42) can now be written as

$$\frac{\partial \mathbf{u}'}{\partial \bar{t}} + \beta \frac{\partial [\mathbf{F}_{1}(\mathbf{u}) - \mathbf{F}_{1}(\bar{\mathbf{u}}_{p})]}{\partial \bar{t}} + (\sigma_{x} + \sigma_{y})\mathbf{u}'
+ (\sigma_{x} + \sigma_{y})\beta [\mathbf{F}_{1}(\mathbf{u}) - \mathbf{F}_{1}(\bar{\mathbf{u}}_{p})] + \sigma_{x}\sigma_{y}\mathbf{q} + \sigma_{x}\sigma_{y}\beta\mathbf{q}_{1}
+ \frac{\partial [\mathbf{F}_{1}(\mathbf{u}) - \mathbf{F}_{1}(\bar{\mathbf{u}}_{p})]}{\partial x} + \frac{\partial [\mathbf{F}_{2}(\mathbf{u}) - \mathbf{F}_{2}(\bar{\mathbf{u}}_{p})]}{\partial y}
+ \sigma_{y}\frac{\partial \mathbf{q}_{1}}{\partial x} + \sigma_{x}\frac{\partial \mathbf{q}_{2}}{\partial y} = 0$$
(46)

In the original space and time variables x, y and t, we get

$$\frac{\partial \mathbf{u}'}{\partial t} + \frac{\partial [\mathbf{F}_{1}(\mathbf{u}) - \mathbf{F}_{1}(\bar{\mathbf{u}}_{p})]}{\partial x} + \frac{\partial [\mathbf{F}_{2}(\mathbf{u}) - \mathbf{F}_{2}(\bar{\mathbf{u}}_{p})]}{\partial y}
+ \sigma_{y} \frac{\partial \mathbf{q}_{1}}{\partial x} + \sigma_{x} \frac{\partial \mathbf{q}_{2}}{\partial y} + (\sigma_{x} + \sigma_{y})\mathbf{u}' + \sigma_{x}\beta[\mathbf{F}_{1}(u) - \mathbf{F}_{1}(\bar{\mathbf{u}}_{p})]
+ \sigma_{x}\sigma_{y}\mathbf{q} + \sigma_{x}\sigma_{y}\beta\mathbf{q}_{1} = 0$$

Since the pseudo mean-flow is time-independent and satisfies the steady Euler equation, we have the following PML equation written in the original total variable **u**,

$$\frac{\partial \mathbf{u}}{\partial t} + \frac{\partial \mathbf{F}_{1}(\mathbf{u})}{\partial x} + \frac{\partial \mathbf{F}_{2}(\mathbf{u})}{\partial y} + \sigma_{y} \frac{\partial \mathbf{q}_{1}}{\partial x} + \sigma_{x} \frac{\partial \mathbf{q}_{2}}{\partial y}
+ (\sigma_{x} + \sigma_{y})(\mathbf{u} - \bar{\mathbf{u}}_{p}) + \sigma_{x} \beta [\mathbf{F}_{1}(\mathbf{u}) - \mathbf{F}_{1}(\bar{\mathbf{u}}_{p})]
+ \sigma_{x} \sigma_{y} \mathbf{q} + \sigma_{x} \sigma_{y} \beta \mathbf{q}_{1} = 0$$
(47)

Eqs. (47) and (43)–(45) are to be solved in the PML domain.

Before presenting a different way of deriving the time-domain equations, we note that, first, upon linearization about $\bar{\mathbf{u}}_p$, the above can be shown to be equivalent to the PML for the linearized Euler equations with a non-uniform mean-flow given in [14]. Second, there are three sets of auxiliary variables introduced in the PML domain, which could increase computational storage and cost. For this reason, we next consider a split approach in forming the time-domain PML equation in which only one set of auxiliary variable is necessary.

4.2. Split version

In the split approach, we re-write the frequency domain PML (41) in two equations as follows, similar to what was done in the original PML formulation [5,16],

$$(-i\bar{\omega})(\bar{\mathbf{u}}_{1}'+\beta[\mathbf{F}_{1}(\mathbf{u})\widetilde{-\mathbf{F}_{1}}(\bar{\mathbf{u}}_{p})])+\frac{1}{1+i\frac{\sigma_{x}}{\bar{\omega}}}\frac{\partial[\mathbf{F}_{1}(\mathbf{u})\widetilde{-\mathbf{F}_{1}}(\bar{\mathbf{u}}_{p})]}{\partial x}=0$$
(48)

$$(-i\bar{\omega})\bar{\mathbf{u}}_{2}^{\prime} + \frac{1}{1 + i\frac{\sigma_{y}}{\bar{\omega}}} \frac{\widehat{\partial}\left[\mathbf{F}_{2}(\mathbf{u}) - \mathbf{F}_{2}(\bar{\mathbf{u}}_{p})\right]}{\widehat{\partial}y} = 0$$

$$(49)$$

where we have

$$\mathbf{u}' = \mathbf{u}_1' + \mathbf{u}_2' \tag{50}$$

As we can see, by adding the two Eqs. (48) and (49), we will recover (41). To write the above in the time domain, we multiply $\left(1+i\frac{\sigma_x}{\bar{\omega}}\right)$ and $\left(1+i\frac{\sigma_y}{\bar{\omega}}\right)$ to (48) and (49), respectively, and get

$$\begin{split} &(-i\bar{\omega}+\sigma_x)(\bar{\mathbf{u}}_1'+\beta[\mathbf{F}_1(\mathbf{u})\widetilde{-\mathbf{F}}_1(\bar{\mathbf{u}}_p)])+\frac{\partial[\mathbf{F}_1(\mathbf{u})\widetilde{-\mathbf{F}}_1(\bar{\mathbf{u}}_p)]}{\partial x}=0\\ &(-i\bar{\omega}+\sigma_y)\bar{\mathbf{u}}_2'+\frac{\partial[\mathbf{F}_2(\mathbf{u})\widetilde{-\mathbf{F}}_2(\bar{\mathbf{u}}_p)]}{\partial x}=0 \end{split}$$

which yields immediately

$$\begin{split} &(-i\bar{\omega})(\bar{\mathbf{u}}_1'+\beta[\mathbf{F}_1(\mathbf{u})\widetilde{-\mathbf{F}}_1(\bar{\mathbf{u}}_p)])+\sigma_x(\bar{\mathbf{u}}_1'+\beta[\mathbf{F}_1(\mathbf{u})\widetilde{-\mathbf{F}}_1(\bar{\mathbf{u}}_p)])\\ &+\frac{\partial[\mathbf{F}_1(\mathbf{u})\widetilde{-\mathbf{F}}_1(\bar{\mathbf{u}}_p)]}{\partial x}=0\\ &(-i\bar{\omega})\bar{\mathbf{u}}_2'+\sigma_y\bar{\mathbf{u}}_2'+\frac{\partial[\mathbf{F}_2(\mathbf{u})\widetilde{-\mathbf{F}}_2(\bar{\mathbf{u}}_p)]}{\partial y}=0 \end{split}$$

The above can be written easily in the time domain as

$$\begin{split} &\frac{\partial \mathbf{u}_{1}'}{\partial \bar{t}} + \beta \frac{\partial [\mathbf{F}_{1}(\mathbf{u}) - \mathbf{F}_{1}(\bar{\mathbf{u}}_{p})]}{\partial \bar{t}} + \sigma_{x}(\mathbf{u}_{1}' + \beta [\mathbf{F}_{1}(\mathbf{u}) - \mathbf{F}_{1}(\bar{\mathbf{u}}_{p})]) \\ &+ \frac{\partial [\mathbf{F}_{1}(\mathbf{u}) - \mathbf{F}_{1}(\bar{\mathbf{u}}_{p})]}{\partial x} = 0 \\ &\frac{\partial \mathbf{u}_{2}'}{\partial \bar{t}} + \sigma_{y}\mathbf{u}_{2}' + \frac{\partial [\mathbf{F}_{2}(\mathbf{u}) - \mathbf{F}_{2}(\bar{\mathbf{u}}_{p})]}{\partial y} = 0 \end{split}$$

Finally, in the original space and time variables x, y and t, we get

$$\frac{\partial \mathbf{u}_{1}'}{\partial t} + \sigma_{x}\mathbf{u}_{1}' + \sigma_{x}\beta[\mathbf{F}_{1}(\mathbf{u}) - \mathbf{F}_{1}(\bar{\mathbf{u}}_{p})] + \frac{\partial[\mathbf{F}_{1}(\mathbf{u}) - \mathbf{F}_{1}(\bar{\mathbf{u}}_{p})]}{\partial x} = 0$$
(51)

$$\frac{\partial \mathbf{u}_2'}{\partial t} + \sigma_y \mathbf{u}_2' + \frac{\partial [\mathbf{F}_2(\mathbf{u}) - \mathbf{F}_2(\bar{\mathbf{u}}_p)]}{\partial v} = 0$$
 (52)

These two equations form the PML for absorbing \mathbf{u}' in the PML domain.

We can also re-write these two equations slightly differently for implementational convenience, as was done in some previous PML works [15,26]. By adding (52) to (51) and replacing \mathbf{u}'_1 with $\mathbf{u}' - \mathbf{u}'_2$, (51) may be written alternatively as

$$\frac{\partial \mathbf{u}'}{\partial t} + \sigma_x(\mathbf{u}' - \mathbf{u}_2') + \sigma_y \mathbf{u}_2' + \sigma_x \beta [\mathbf{F}_1(\mathbf{u}) - \mathbf{F}_1(\bar{\mathbf{u}}_p)]
+ \frac{\partial [\mathbf{F}_1(\mathbf{u}) - \mathbf{F}_1(\bar{\mathbf{u}}_p)]}{\partial x} + \frac{\partial [\mathbf{F}_2(\mathbf{u}) - \mathbf{F}_2(\bar{\mathbf{u}}_p)]}{\partial y} = 0$$

Finally, by renaming \mathbf{u}_2 the auxiliary variable \mathbf{q} and noting the fact that $\bar{\mathbf{u}}_p$ is independent of time and satisfies the steady Euler equation, we have the following equations to be used in PML domains.

$$\frac{\partial \mathbf{u}}{\partial t} + \frac{\partial \mathbf{F}_{1}(\mathbf{u})}{\partial x} + \frac{\partial \mathbf{F}_{2}(\mathbf{u})}{\partial y} + \sigma_{x}(\mathbf{u} - \bar{\mathbf{u}}_{p} - \mathbf{q})
+ \sigma_{y}\mathbf{q} + \sigma_{x}\beta[\mathbf{F}_{1}(\mathbf{u}) - \mathbf{F}_{1}(\bar{\mathbf{u}}_{p})] = 0$$
(53)

$$\frac{\partial \mathbf{q}}{\partial t} + \sigma_{y} \mathbf{q} + \frac{\partial [\mathbf{F}_{2}(\mathbf{u}) - \mathbf{F}_{2}(\bar{\mathbf{u}}_{p})]}{\partial y} = 0$$
 (54)

In this way, only one auxiliary variable, \mathbf{q} , is necessary.

For a numerical example, we present a simulation of roll-up vortices of a shear flow induced by the Kelvin–Helmholtz instability, and use PML as the absorbing boundary condition as the vortices convect out of the computational domain. The entire computational domain is $[-1.5, 9.5] \times [-1.1, 1.1]$ with $\Delta x = 0.05$ and $\Delta y = 0.01$, including the surrounding PML domain with a width of 10 grid points. A smaller grid size is used in the *y* direction in order to better resolve the shear flow. The non-linear Euler Eq. (33) is solved in the interior physical domain and the PML Eqs. (53) and (54) are solved in the PML domain.

The initial condition in primitive variables is

$$\begin{pmatrix} \rho \\ u \\ v \\ p \end{pmatrix} = \begin{pmatrix} \overline{\rho}(y) \\ \overline{U}(y) \\ 0 \\ \frac{1}{y} \end{pmatrix}$$
 (55)

where

$$\overline{U}(y) = \frac{1}{2} \left[(U_1 + U_2) + (U_1 - U_2) \tanh\left(\frac{2y}{\delta}\right) \right]$$
 (56)

and

$$\bar{\rho}(y) = \frac{1}{\bar{T}(y)} \tag{57}$$

with

$$\bar{T}(y) = T1 \frac{\overline{U} - U_2}{U_1 - U_2} + T_2 \frac{U_1 - \overline{U}}{U_1 - U_2} + \frac{\gamma - 1}{2} (U_1 - \overline{U})(\overline{U} - U_2)$$
(58)

where the mean temperature $\bar{T}(y)$ is determined by the Crocco relation for compressible flows. The parameters are

$$U_1 = 0.8, \quad U_2 = 0.2, \quad \delta = 0.4,$$

 $T_1 = 1, \quad T_2 = 0.8, \quad \gamma = 1.4$

A source term is added to the energy equation in (33) to induce the instability wave. The source term is of the form

$$s(x, y, t) = 5\sin(\omega t)e^{-(\ln 2)[(x-x_0)^2 + (y-y_0)^2]/r_0^2}$$

where $\omega = \pi/2$, $(x_0, y_0) = (-0.5, 0)$ and $r_0 = 0.03$.

The source term will excite the Kelvin–Helmholtz instability wave which will grow exponentially and then develop into roll-up vortices. The vortices at the out-flow boundary, as well as the acoustic waves at all four artificial boundaries, are to be absorbed by the PML. The pseudo mean-flow $\bar{\mathbf{u}}_p$ used in the PML equation is the same parallel flow as that of the initial condition (55). The linear wave analysis for this particular shear flow has been carried out in [14], where the value for β was found to be approximately 1/1.4. Fig. 10 shows vorticity contours at progressive time frames as the roll-up vortices exit the outflow boundary. As the vortices convect downstream, they are absorbed exponentially in the PML domain. No numerical instability is observed.

In Fig. 11, we compare time history of v velocity component at a point close to the outflow boundary with that of a larger domain computation. The numerical solution is plotted in the solid line and the larger domain calculation in circles. Very little differences were found. This confirms the effectiveness of PML in truncating the outflow boundary in a non-linear simulation.

It is also possible to use a different pseudo mean-flow at the outflow boundary. In addition to the initial condition

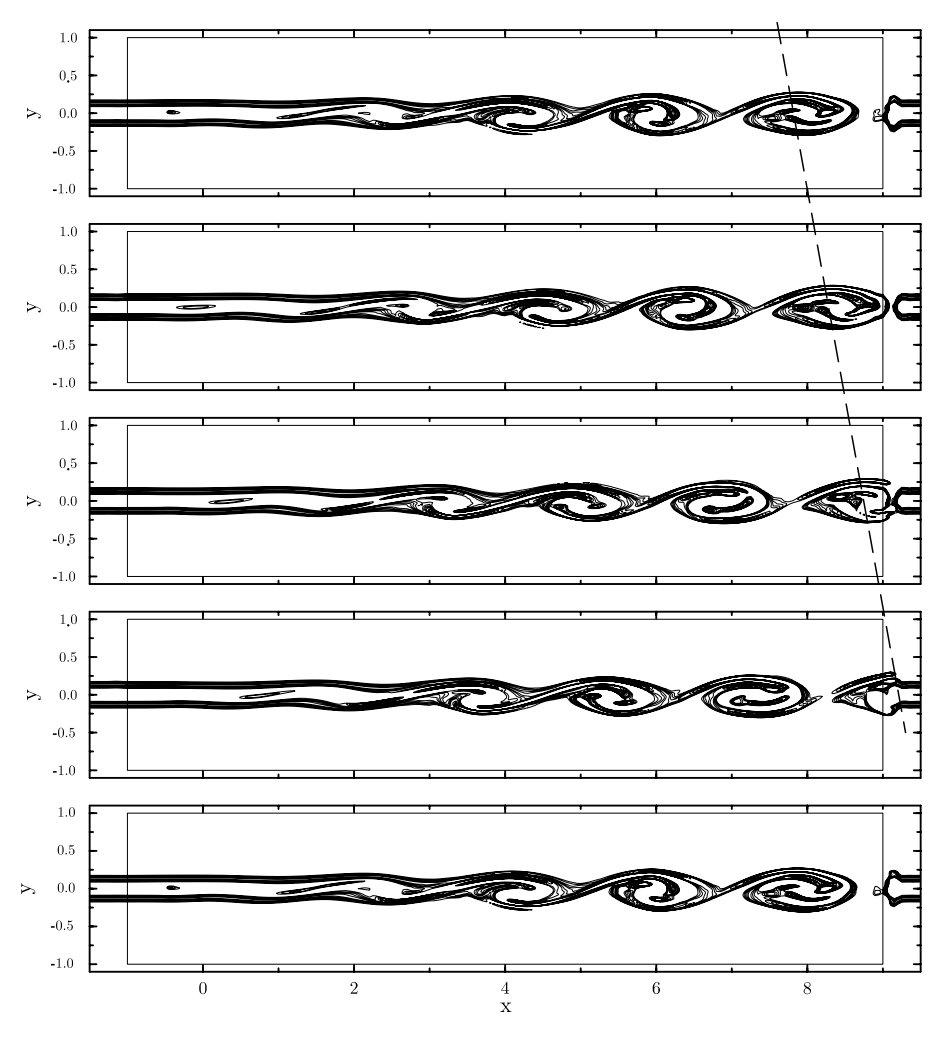


Fig. 10. Vorticity contours in progressive time frames.

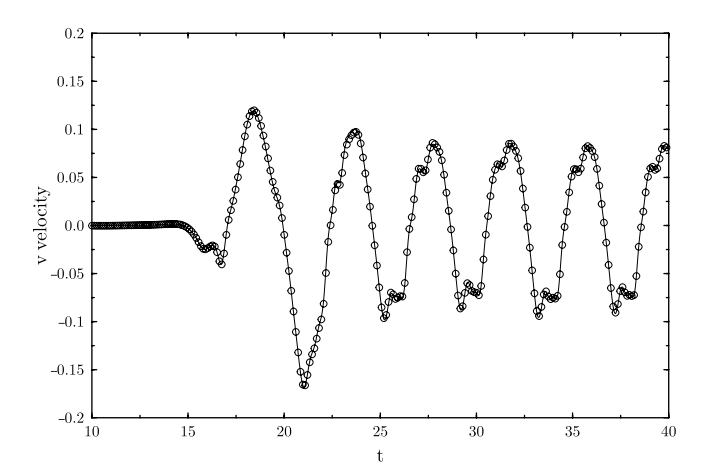


Fig. 11. velocity v as a function of time at a point close to the outflow boundary, (x, y) = (8.75, 0.5). Solid line: computational; circle: larger domain calculation

(55) as pseudo mean-flow in the PML equations, parallel flows of $\overline{U}(y)$ in the form of (56) with $\delta=0.6$ and $\delta=0.8$ have also been tested. Fig. 12 shows the instantaneous u velocity contours obtained using three different pseudo mean-flow profiles. The results are very close which implies that all three pseudo mean-flows are viable choices for the PML equations.

More examples of PML for the non-linear Euler equation can be found in [21].

5. Concluding remarks

From the linearized Euler equations with a uniform mean-flow, to a non-uniform mean-flow, to the fully

non-linear Euler equations, the PML technique has been successfully applied to a broad class of problems in Computational Aeroacoustics as a non-reflecting boundary condition. In this paper, recent developments are reviewed. The importance of a proper space—time transformation in the process of deriving the PML equations is emphasized through the view point of PML as complex change of variables. Three essential steps in the construction of PML are outlined and illustrated by examples for the linearized and non-linear Euler equations, with numerical examples.

The presentation of the PML technique in this review has been focused on the view that the PML technique is essentially a complex change of variable in the frequency domain. There are however other approaches in the literature on deriving the PML equations. In [3,12], different, but somewhat equivalent, ways of constructing the PML equations were offered. And recently, in [24], a new approach of formulating the PML based on a factorization of the Euler system was given.

PML for Computational Fluid Dynamics and Computational Aeroacoustics is still an active area of research. Further applications of the PML technique are being explored. Some of the unanswered questions are: how to formulate stable PML with a mean flow in an arbitrary direction? Is there a simple and direct formula for determining the parameter β for an arbitrarily given mean flow? How to formulate PML for transonic mean flows? What are the stability properties of the non-linear PML equations? How to extend the PML to non-linear Navier—Stokes equations and what are the physical and non-physical effects of using PML in a turbulence simulation? We hope these questions will be answered in future studies.

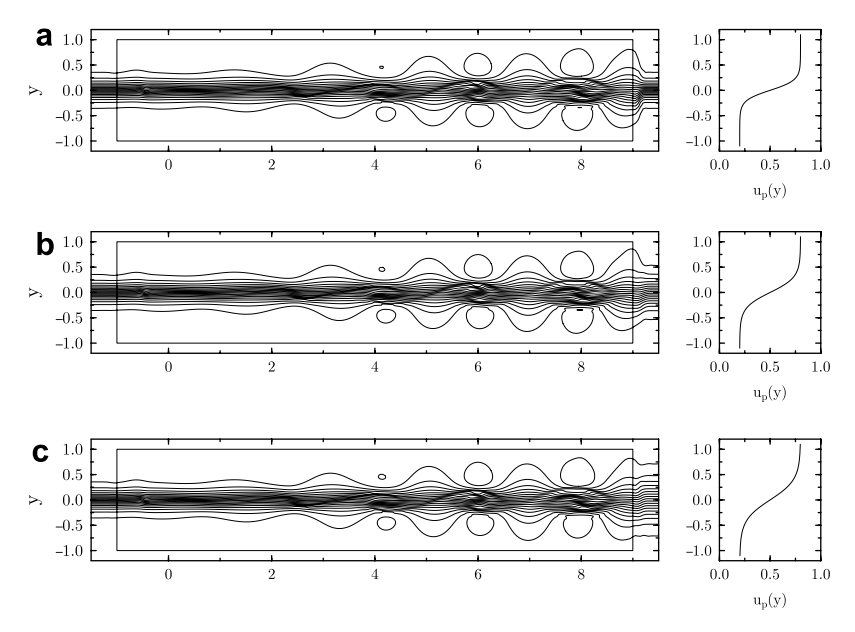


Fig. 12. Instantaneous contours of the u velocity and the pseudo mean velocity profile used in the PML equation at the outflow boundary: (a) $\delta = 0.4$; (b) $\delta = 0.6$ and (c) $\delta = 0.8$.

Acknowledgement

This work is supported by a grant from the National Science Foundation DMS-0411402.

References

- Abarbanel S, Gottlieb D. A mathematical analysis of the PML method. J Comput Phys 1997;134:357.
- [2] Bayliss A, Turkel E. Radiation boundary conditions for wave-like equations. Commun on Pure Appl Math 1980;33:708–25.
- [3] Becache E, Bonnet-Ben Dhia A-S, Legendre G. Perfectly matched layers for the convected Helmholtz equation. SIAM J Numer Anal 2004;42(1):409–33.
- [4] Becache E, Fauqueux S, Joly P. Stability of perfectly matched layers, group velocities and anisotropic waves. J Comput Phys 2003;188:399–433.
- [5] Berenger JP. A perfectly matched layer for the absorption of electromagnetic waves. J Comput Phys 1994;114:185–200.
- [6] Bodony DJ. Analysis of sponge zones for computational fluid mechanics. J Comp Phys 2006;212:681–702.
- [7] Chew WC, Weedon WH. A 3D perfectly matched medium from modified Maxwell's equations with stretched coordinates. IEEE Microwave Opt Technol Lett 1994;7:599–604.
- [8] Collino F, Monk P. The perfectly matched layer in curvilinear coordinates. SIAM J Sci Comp 1998;19(6):2016.
- [9] Dahl MD. Fourth Computational Aeroacoustics (CAA) Workshop on Benchmark Problems. NASA CP-2004-212954, 2004.
- [10] Gedney SD. An anisotropic perfectly matched layer-absorbing medium for the truncation of FDTD lattices. IEEE Trans Antennas Propagation 1996;44:1630.
- [11] Giles MB. Non-reflecting boundary conditions for Euler equation calculations. AIAA J 1990;28:2050–8.
- [12] Hagstrom T, Nazarov I. Absorbing layers and radiation boundary conditions for jet flow simulations. AIAA paper 2002-2606, 2002.
- [13] Hagstrom T, Nazarov I. Perfectly matched layers and radiation boundary conditions for shear flow calculations. AIAA paper 2003-3298, 2003.
- [14] Hagstrom T, Goodrich J, Nazarov I, Dodson C. High-order methods and boundary conditions for simulating subsonic flows AIAA paper 2005-2869, 2005.
- [15] Hayder ME, Atkins HL. In: Geers TL, editor. Experiences with PML boundary conditions in fluid-flow computations, IUTAM symposium

- of computational methods for unbounded domains. Kluwer Academic Publishers; 1998. p. 207–16.
- [16] Hu FQ. On absorbing boundary conditions of linearized Euler equations by a perfectly matched layer. J Comput Phys 1996;129:201–19.
- [17] Hu FQ. On perfectly matched layer as an absorbing boundary condition. AIAA paper 96-1664, 1996.
- [18] Hu FQ. A stable, perfectly matched layer for linearized Euler equations in unsplit physical variables. J Comput Phys 2001;173:455–80.
- [19] Hu FQ. Absorbing boundary conditions (a review). Int J Comput Fluid Dyn 2004;18(6):513–22.
- [20] Hu FQ. A perfectly matched layer absorbing boundary condition for linearized Euler equations with a non-uniform mean-flow. J Comput Phys 2005;208:469–92.
- [21] Hu FQ. On the construction of PML absorbing boundary condition for the non-linear Euler equations. AIAA paper 2006-0798, 2006.
- [22] Hu FQ, Hussaini MY, Manthey JL. Low-dissipation and -dispersion Runge-Kutta schemes for computational acoustics. J Comput Phys 1996;124:177–91.
- [23] Mack LM. On the invicid acoustic-mode instability of supersonic shear flows. Theoret Comput Fluid Dyn 1990;2:97–123.
- [24] Nataf F. A new approach to perfectly matched layers for the linearized Euler system. J Comput Phys 2006;214(2):757–72.
- [25] Poinsot T, Lele SK. Boundary conditions for direct simulation of compressible viscous flows. J Comput Phys 1992;101:104–29.
- [26] Tam CKW, Auriault L, Cambulli F. Perfectly matched layer as an absorbing boundary condition for the linearized Euler equations in open and ducted domains. J Comput Phys 1998;144:213–34.
- [27] Tam CKW, Hu FQ. On the three families of instability waves of highspeed jets. J Fluid Mech 1989;201:447–83.
- [28] Tam CKW, Webb JC. Dispersion-relation-preserving schemes for computational acoustics. J Comput Phys 1993;107:262–81.
- [29] Thompson KW. Time-dependent boundary conditions for hyperbolic systems. J Comput Phys 1987;68:1–24.
- [30] Turkel E, Yefet A. Absorbing PML boundary layers for wave-like equations. Appl Numer Math 1998;27:533–57.
- [31] Zhao L, Cangellaris AC. GT-PML: generalized theory of perfectly matched layers and its application to the reflectionless truncation of finite-difference time-domain grids. IEEE Trans Microwave Theory Tech 1996;44:2555–63.
- [32] Whitman GB. Linear and nonlinear waves. Willey; 1978.